ACS APPLIED BIO MATERIALS

www.acsabm.org Article

Simultaneous Determination of L-Phenylalanine, Phenylethylamine, and Phenylacetic Acid Using Three-Color Whole-Cell Biosensors within a Microchannel Device

Li-Wen Hsu, Yu-Hsuan Lin, Jun-Yu Guo, Chien-Fu Chen, Yi-Ju Chou, and Yi-Chun Yeh*

Cite This: https://dx.doi.org/10.1021/acsabm.0c00590 Read Online

ACCESS | Metrics & More | Article Recommendations | Supporting Information

ABSTRACT: The neurotransmitter phenylethylamine (PEA) is highly susceptible to oxidation to produce phenylacetic acid (PA). The fact that PEA and PA are both metabolites of phenylalanine (Phe) in humans makes them important indicators in the diagnosis of phenylketonuria. In this work, three-color whole-cell biosensors were developed to simultaneously detect these analytes (Phe, PEA, and PA). The tyrosine-responsive promoter was used to control the production of green fluorescent protein signals in response to Phe levels. The FeaR regulon was first used to indicate the presence of PEA, whereas the Paa regulon was used for the detection of PA. The combination of three sensor strains together made it possible to semiquantify the three analytes according to unique color outputs without cross-interference. We sought to optimize various modular components (ribosomal binding sites and fluorescent proteins) to ensure the rapid generation of fluorescent signals. Finally, the biosensors were implemented within a microchannel device to reduce sample consumption in point-of-care assays.

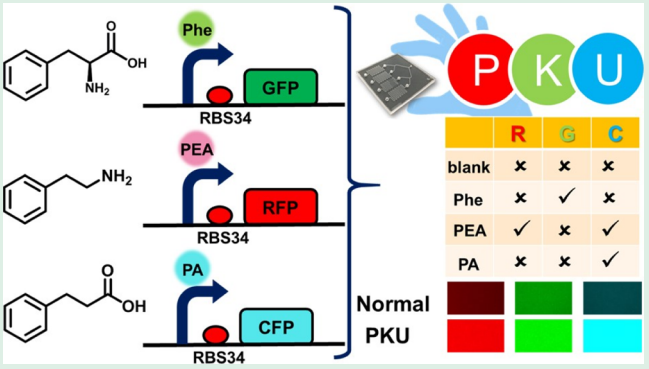

KEYWORDS: *phenylketonuria (PKU), whole-cell biosensor, phenylalanine, phenylethylamine, phenylacetic acid, microfluidic device*

1. INTRODUCTION

Phenylketonuria (PKU) is an inherited disorder involving the metabolism of amino acids. It is caused by a genetic defect of phenylalanine hydroxylase (PAH), a hepatic enzyme that converts phenylalanine (Phe) to tyrosine (Tyr).[1] In the absence of PAH, Phe levels in the blood increase, resulting in the formation of toxic metabolites, including phenylpyruvate (PPA) and phenylacetic acid (PA) (Scheme 1A),[2] which can cause irreversible brain damage.[3] In Europe, PKU occurs in 1/10,000 babies yearly.[4] Treatment for PKU focuses primarily on avoiding the uptake of Phe-rich foods, and dietary control is monitored by assessing the levels of Phe and its metabolites in patients' urine.[5]

Many methods have been reported for the detection of Phe and PA, such as capillary electrophoresis, mass spectrometric methods, and high-performance liquid chromatography.[6−12] However, these analysis methods require tedious sample preparation as well as expensive equipment and may not be suitable for immediate diagnosis. In previous work, our laboratory has developed a whole-cell biosensor to simultaneously detect Phe and Tyr.[13−15] However, the measurements were acquired from 24 h postinduction, which is not suitable for real-time monitoring. In addition, multiplexed detection of a panel of metabolites is crucial for making clinical decisions for real applications.

Escherichia coli uses different transcriptional regulators for controlling the degradation pathways of various aromatic compounds.[16] For example, FeaR and PaaX are two regulatory proteins that recognize aromatic amines and PA, respectively. In *E. coli*, the metabolism of aromatic amines [such as phenylethylamine (PEA), tyramine, and dopamine] requires the production of FeaR-activating proteins (TynA: amine oxidase and FeaB: PAL dehydrogenase) during carbon or nitrogen limitation.[16−20] Thus, PEA is quickly oxidized to the major metabolite, PA, which is a common carbon and energy source for bacteria. For the biosynthesis, uptake, and degradation of aromatic amino acids (Tyr, Phe, and tryptophan),[21−23] the transcriptional regulator TyrR protein plays an essential role in the transcriptional activation/repression (via the formation of dimer and hexamer forms).[21,24−29] The dimer TyrR regulates the activation of *tyrP* (encodes a tyrosine transporter) and *mtr* (encodes a

Received: May 19, 2020
Accepted: July 15, 2020
Published: July 15, 2020

Scheme 1. Schematic Representation of (A) Metabolic Pathways of Phe in Humansa (B) The Genetic Organization of Biosensors[a]

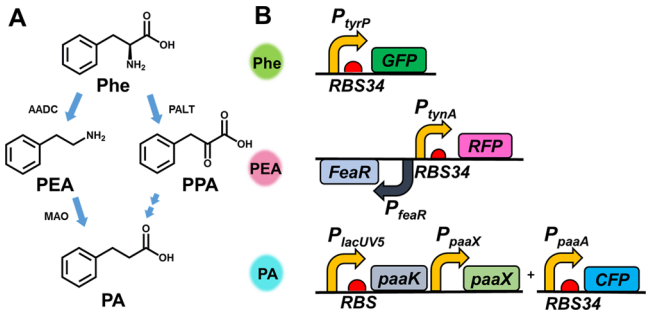

[a]Phe is metabolized to PEA/PPA and finally to PA by various enzymes. AADC (aromatic amino acid decarboxylase), PALT (phenylalanine aminotransferase), and MAO (monoamine oxidase).[33] PA was generated from PPA as well under the catalysis of multienzymes (decarboxylase and dehydrogenase).[34] (B) Proposed sensors were designed based on regulatory proteins including TyrR, FeaR, and PaaX. TyrR-regulated promoter (PtyrP) was used to activate the expression of GFP for reporting the presence of Phe. FeaR-regulated promoter (PtynA) was used to drive the expression of RFP for reporting the presence of PEA. Finally, the PaaX-regulated promoter (PpaaA) was used to activate the expression of CFP for reporting the presence of PA.

tryptophan-specific permease) in the presence of Phe. Moreover, TyrR dimers form hexamers, which regulate the repression of a series of genes in the presence of Tyr. Among Phe-responsive promoters (tyrP and mtr), PtyrP is more specific to the substrates.[13]

In this study, we have developed the first ever whole-cell biosensors capable of simultaneously estimating the concentrations of Phe and its metabolites (PEA and PA) using three-color outputs (Scheme 1B). We optimized a variety of modular components (ribosomal binding sites and fluorescent proteins) to ensure the rapid generation of fluorescent signals to greatly reduce the time necessary for testing from 24 to 5 h. The proposed whole-cell sensors proved successful in the analysis of urine samples without the need for pretreatment. Finally, we implemented the sensors within a microchannel chip to minimize reagent consumption while maximizing portability. Despite a simple design, the proposed device provides good specificity and sensitivity.

2. MATERIALS AND METHODS

2.1. Bacterial Strains, Media, Cultivation, and Plasmid Construction. The cells were initially cultured in LB broth and grown overnight at 37 °C. The cells were then diluted (4%) in M9 medium. The M9 medium was supplemented with 5 mg/mL thiamine hydrochloride (Sigma-Aldrich), 11.1 μg/mL calcium chloride (Ferak Berlin GmbH), 0.24 mg/mL magnesium sulfate (Fisher Chemical), and 2% glycerol (AMRESCO). Both the LB and M9 medium were supplemented with kanamycin at 50 μg/mL (AMRESCO) or chloramphenicol at 100 μg/mL (AMRESCO).

Bacterial strains, plasmids, and primers used in the current study are listed in Tables S1−S3. Details of the strain/plasmid construction are provided in Table S2. All nucleotide sequences were confirmed through DNA sequencing.

2.2. RFP, GFP, and CFP Quantification. Cells were diluted in M9 medium and incubated at 250 rpm, 37 °C (~OD600 = 0.4). Then, analytes were added to induce the production of the fluorescent protein. The quantitation of optical density (OD600) and fluorescence intensity was done at indicated time points. After induction, cell cultures (300 μL) were transferred to a microplate. The OD600 value and the fluorescence intensity were measured in a microplate reader Synergy HT (BioTek, VT) with the photomultiplier tube gain set to 35, using excitation/emission at 530 nm/590 nm (red), 485 nm/528 nm (green), and 420 nm/485 nm (cyan). Software of the microplate reader is Gen5. Error bars indicate the standard deviation from three independent replicates. Both PEA and PA were purchased from Sigma-Aldrich and dissolved in ethanol (Fisher ACS Grade, 99.5%). Phenylalanine (Acros) was dissolved in ultrapure water (Milli-Q purification system). All samples were freshly prepared. For urine analysis, artificial urine (Scientech Corporation) was diluted 5× with M9 medium. The artificial urine was centrifuged at 12,000*g* for 15 min. The supernatant of the artificial urine was filtered through a 0.2 μm filter. The diagnostic ability was confirmed by creating artificial urine mimics containing normal level (Phe: 150 μM, PEA: 5 μM, and PA: 5 μM) and patient levels (PKU1: Phe: 1250 μM, PEA: 150 μM, and PA: 150 μM; PKU2: Phe: 5000 μM, PEA: 750 μM, and PA: 750 μM). These samples were next diluted 5× with M9 to examine the fluorescence intensity.

2.3. Fabrication of a Microfluidic Device. A microfluidic device was fabricated from two cyclo olefin polymer (COP) chips (ZEONOR 1020R, Japan). The chip size was 5 cm × 5.5 cm × 2 mm (Figure S1). To create a threaded screw interface at the syringe port, the top cover chip was drilled using an end mill at 650 μm diameter and a threaded 22 gauge needle.[30] To drill holes on the analyte walls and detection zones, a drill bit with 2.0 mm diameter was used. The bottom chip was next patterned with the serpentine reaction channels and chaotic micromixers. They were then milled onto a bare COP chip using an end mill with a 300 μm diameter using a computer numerical control milling machine (EGX 400, USA). The channel depth was 200 μm, and the micromixer component was made by drilling 300 μm deep holes every 800 μm from the detection zone to the 2/3 length of each flow channel. The COP chip was then sonicated for 30 min in ultrapure water to remove debris and sequentially rinsed with methanol, 2-propanol, and ultrapure water. The cleaned COP chip was dried with nitrogen and deaerated at 50 °C in a vacuum oven for 8 h. Finally, the two chips were sealed together as described in previous work.[30]

2.4. Microchannel Device and Fluorescence Microscopy. For the microfluidic chip, we added 5 μL of analytes to the four microwells in the upper row, subsequently sealed them with a blue tape, and injected 100 μL of the solutions containing sensor cells into the chip with a flow rate (1 mL/min) with a syringe pump (Legato 111, KD Scientific). The sensor cells were implemented in the chip and induced at 37 °C for 5 h. Fluorescence microscopy was performed on an Axio A1 microscope (Carl Zeiss) with an A-Plan 10×/0.25 Ph1. Phase contrast images were obtained using an EC Plan-Neofluar 100×/1.30 and an oil PH3 objective. Images were captured and false-colored using Zeiss ZEN software (all from Carl Zeiss Microscopy). Red fluorescent protein (RFP) images were false-colored red, green fluorescent protein (GFP) images were false-colored green, and cyan fluorescent protein (CFP) images were false-colored cyan. Sensor cells were grown in the presence of Phe (200 μM), PEA (25 μM), and PA (50 μM) and immobilized in 1% agarose.

3. RESULTS AND DISCUSSION

3.1. Design of Sensor Strains for the Determination of Phe, PEA, and PA. We first used three sensor strains for monitoring the presence of Phe, PEA, and PA, respectively (Figure S2A). The M9 medium containing glycerol was used as the growth medium to avoid glucose repression in PA transcriptional activation.[31] We recorded the end-point fluorescence intensities/OD for each strain in the presence of target analytes relative to that of the untreated cells (blank). Accordingly, the fluorescent signal was observed to increase over this reaction time-course (Figure S2B−D). The intensity increased initially and reached a plateau within approximately 5 h (except for Phe). We therefore recorded data from 5 h

https://dx.doi.org/10.1021/acsabm.0c00590
ACS Appl. Bio Mater. XXXX, XXX, XXX−XXX

postinduction to enable rapid detection with reasonable incubation in all subsequent experiments. TyrR protein levels have been shown to have a dramatic effect on the regulation of TyrR-dependent promoters.[13] Next, we tested the expression of the Phe biosensors on isopropyl β-D-1-thiogalactopyranoside (IPTG) at various concentrations (tuning level of TyrR) using GFP as the output signal (Figure 1A) and found that the concentration of IPTG was inversely proportional to the induction fold and the GFP produced. In other words, the Phe biosensors produced the highest intensity of GFP in the absence of IPTG. We speculated that the chromosomal expression in *E. coli* produced sufficient TyrR regulatory protein to enable binding to Phe to subsequently produce GFP under environmental conditions. We next examined the induction of PtyrP in the presence of Phe without the expression of tyrR on the same plasmid. Figure 1B shows a comparison of the end-point GFP intensity/OD and induction folds in the cells in the presence of Phe at 200 μM. Similarly, sensor cells present a higher intensity of GFP without extra copies of TyrR. Notably, the basal expression levels are elevated as well, indicating that TyrR protein levels have a dramatic impact on the regulation of PtyrP. Thus, we settled on the strain without extra TyrR copies based on high-signal intensities. The PA biosensor also produced the largest quantity of GFP in the absence of IPTG (Figure 1C). This result is consistent with our previous work that the activation of PpaaA remains at the basal level of PaaK.[15]

3.2. Selection of Ribosome-Binding Sites and Fluorescent Proteins for Phe, PEA, and PA Biosensors. The difference between ribosome-binding sites (RBSs) in their ability to bind to ribosomes can affect the number of proteins that are subsequently transcribed.[32] In the current study, a comparison of the sequences of RBS34 and RBS10 (Figure S3) deemed the former the optimal RBS sequence, as it produced fluorescence of greater intensity in all three of our biosensors, resulting in higher sensitivity sensors.

We then systematically replaced each of the biosensors with a different fluorescent protein. The three Phe biosensors developed in this study (using CFP, GFP, and RFP) provided similar performance in terms of Phe induction (Figure 2A); however, the GFP signal is the strongest among the three, therefore we settled on using GFP in our Phe biosensors. The PEA biosensors using RFP as a signal output produced the most substantial fluorescence and induction ratio (Figure 2B). PA biosensors using both GFP and CFP presented great fluorescence performance and induction ratios (Figure 2C). Taken together, these results led us to conclude that the optimal fluorescent protein outputs for quantifying Phe, PEA, and PA levels were green, red, and cyan fluorescent proteins.

We then performed the experiments to evaluate the dose–response relationships between fluorescence intensities/OD values at various analyte concentrations at 5 h postinduction for three sensor strains (Figure 2D–F). The fluorescence microscopy photograph indicates the substrate-dependent fluorescence intensity increase with various concentrations. Under optimal experimental conditions, the fluorescence intensities/OD values were shown to increase linearly with the addition of Phe at concentrations of 5–50 μM (Figure S4A). A linear relationship between fluorescence intensities/OD values and the concentration of PEA and PA was observed with the regression coefficient R^2 = 0.962 and 0.981 and an LOD at 1.05 and 0.22 μM, respectively (Figure S4B,C).

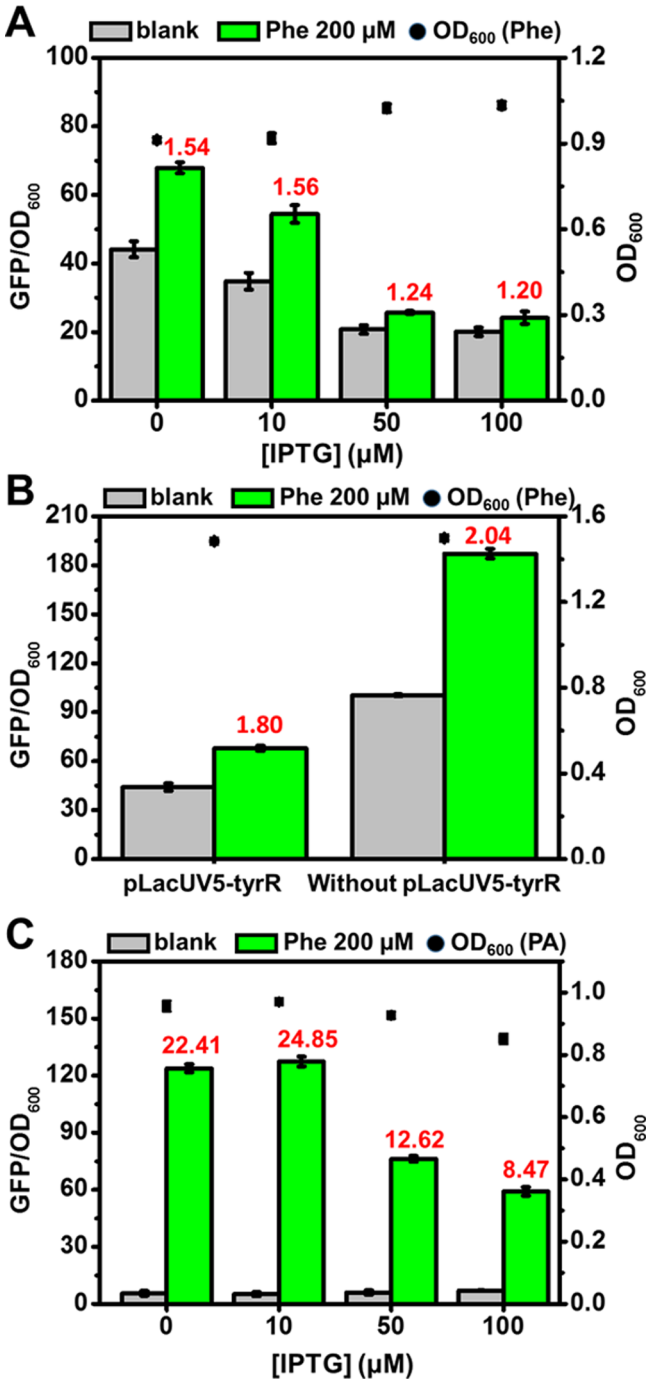

Figure 1. (A) Fluorescence intensity and OD600 of the Phe biosensor in the presence of Phe at 200 μM and various concentrations of IPTG at 5 h postinduction. (B) Without the pLacUV5-tyrR gene, the tyrP promoter retains the expression of GFP in the presence of Phe. (C) Fluorescence intensity and OD600 of the PA biosensor in the presence of PA at 50 μM and various concentrations of IPTG at 5 h postinduction. The numbers in red indicate the induction folds relative to untreated controls.

3.3. Determining Substrate Specificity. The three sensor strains (Phe@GFP, PEA@RFP, and PA@CFP) were then mixed together at a 1:1:1 volume ratio and cocultured for the simultaneous semiquantification of Phe, PEA, and PA. Quantification was done by analyzing the three fluorescent signals whose intensities were proportional to the amounts of target analytes present in the test sample. The cross-

https://dx.doi.org/10.1021/acsabm.0c00590
ACS Appl. Bio Mater. XXXX, XXX, XXX–XXX

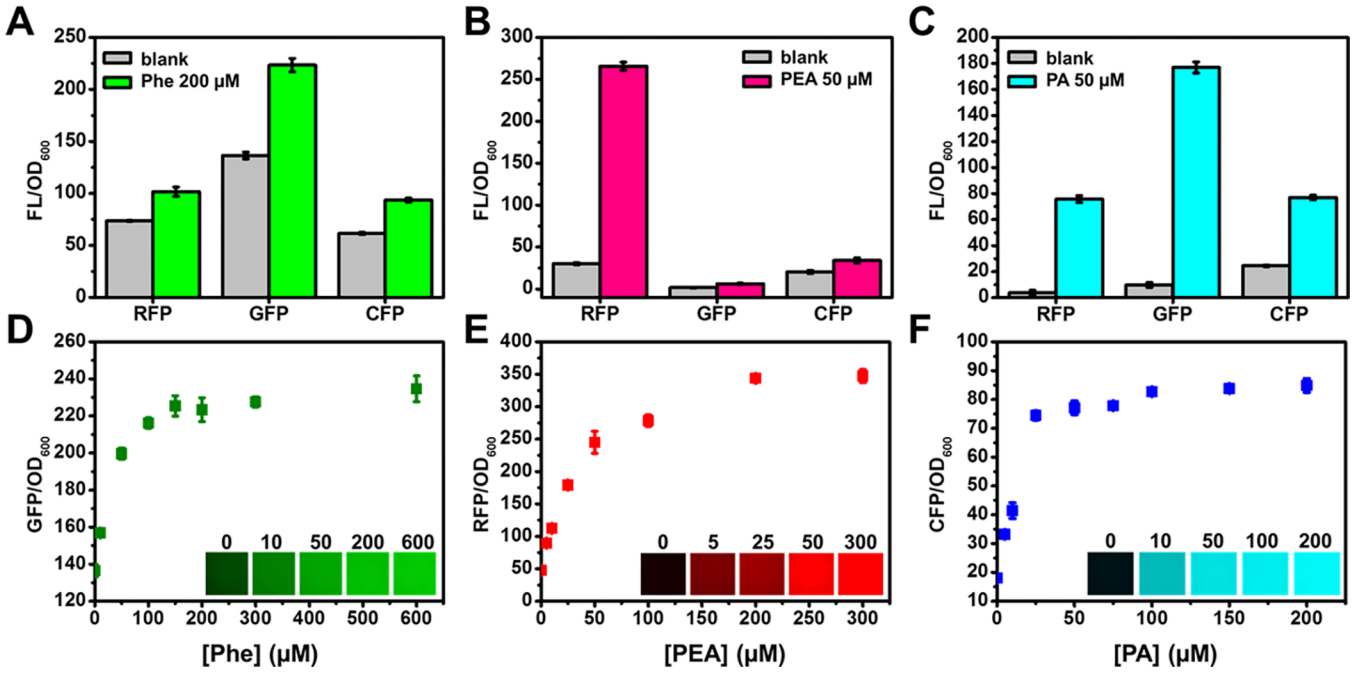

Figure 2. (A–C) Comparison of three fluorescent protein expression levels (RFP, GFP, and CFP) in sensor cells in the presence of target analytes. (D–F) Dose–response relationships of three biosensor cells in the presence of target analytes at 5 h postinduction. The inset fluorescence microscopy pictures show the imaging of sensor cells at different substrate concentrations.

interference of the cocultured biosensors was evaluated by supplementing the reaction medium with a mixture of interfering substrates including Phe (200 μM), PEA (25 μM), and PA (50 μM) (Figure 3A). Mixtures of three-color whole-cell biosensors showed significant induction in response to the presence of the corresponding substrates. It was found that the copresence of PEA increased the intensity of the CFP signals because of the conversions of PEA to PA (PA: end products of PEA metabolism). These results are consistent with earlier studies showing that PA was produced by PEA at concentrations higher than 10 μM; however, low urinary PEA levels are commonly observed for healthy individuals. Thus, it should be negligible to interfere with the analysis of biological samples.

Phase-contrast and fluorescence microscopy images of cells comprising mixtures of three-color whole-cell biosensors were examined (Figure 3B). Single-cell assays containing three substrates were highly consistent with the results of solution.

3.4. Applications in Real-Sample Analysis on Microfluidics. To enhance the user convenience, the sensor cells were implemented in a microfluidic chip to enable observation under a fluorescence microscope. We spotted the samples containing Phe at 50 μM in the microwells to test the robustness of our devices for replicates (Figure 4A). The syringe containing a mixture of three-color whole-cell biosensors was injected and flowed into the microfluidic channel with a flow rate of 1 mL/min. Fluorescence image analysis showed nearly identical results among four channels indicating that this device enables a homogeneous cell distribution. We therefore tested one substrate alone (Phe, PEA, and PA) and a mixture of three in four independent microwells. As expected, the performance of the sensor cells within the microfluidic chip was maintained as before (Figure 4B); whereas the high portability, rapid analysis, and low reagent consumption make this device ideal for point-of-care applications.

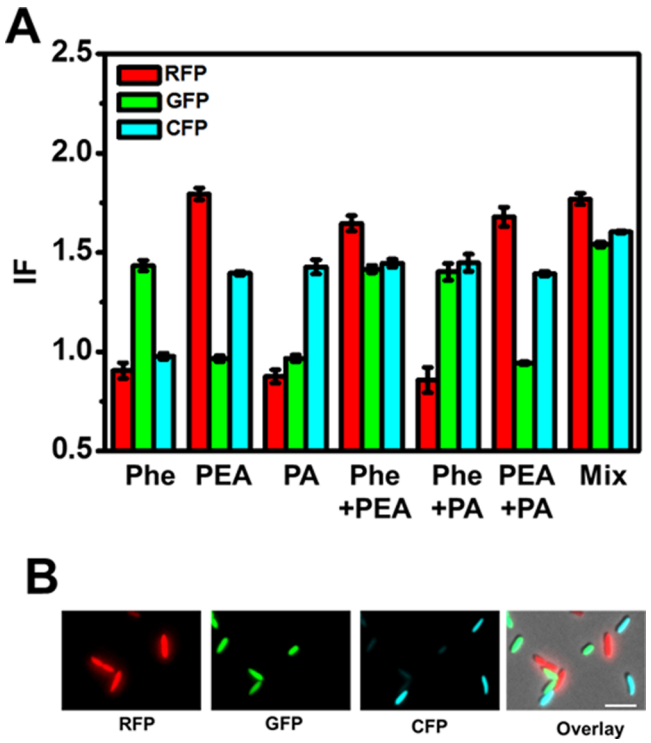

Figure 3. (A) Fluorescence induction relative to untreated controls of the three-color whole-cell mixtures in the presence of one substrate alone (Phe 200 μM, PEA 25 μM, and PA 50 μM), mixture of two substrates, and mixture of three substrates, at 5 h postinduction. (B) Fluorescence microscopy images of the three-color whole-cell mixtures in the copresence of Phe, PEA, and PA (scale bar, 5 μm).

To determine the effectiveness of the proposed sensors in different matrices, artificial urine was used to mimic the properties and composition of real urine. Diagnoses of PKU

https://dx.doi.org/10.1021/acsabm.0c00590
ACS Appl. Bio Mater. XXXX, XXX, XXX–XXX

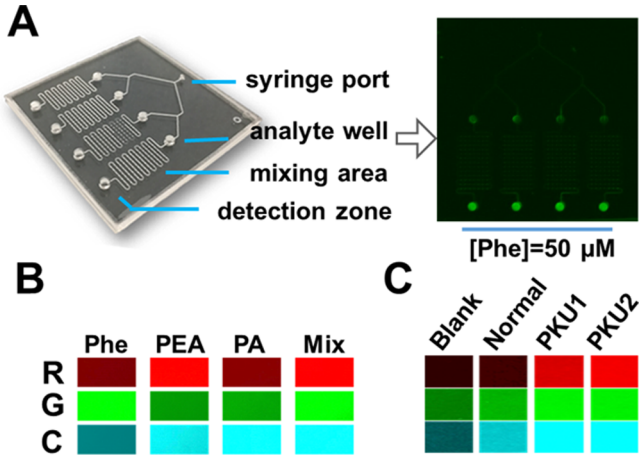

Figure 4. (A) Photo of the microfluidic system and a schematic demonstration (left). The green fluorescence image of three-color whole-cell biosensors within the microfluidic system in the presence of Phe at 50 μM (right). (B) Performance of the three-color whole-cell biosensor cells within the microfluidic chip. Four sample wells contain Phe (200 μM), PEA (25 μM), PA (50 μM), and the mixture of three. Red, green, and cyan fluorescence images were recorded. Images were captured and false-colored using Zeiss ZEN software (all from Carl Zeiss Microscopy). RFP images were false-colored red, GFP images were false-colored green, and CFP images were false-colored cyan. (C) Red, green, and cyan fluorescence images of blank artificial urine, normal, PKU1, and PKU2 mimics.

were done utilizing artificial mimics (PKU1 and PKU2), which were prepared by applying sample solutions containing high levels of Phe, PEA, and PA in buffer/artificial urine. We diluted the urine sample 5× using M9 medium to ensure that the detection range of the sensor cells falls within a set of clinical range. As shown in Figures 4C and S5, induction folds and images were statistically significantly higher in patients, indicating that a rapid home monitor assay for dietary assessments and adjustment could be achieved under current settings.

4. CONCLUSIONS

In summary, we have developed three-color whole-cell biosensors capable of semiquantifying Phe, PEA, and PA levels simultaneously. When the analyte levels exceeded a threshold concentration level, the biosensors presented a noticeable color change. The biosensors developed in this study enable the detection of Phe, PEA, and PA with a high degree of sensitivity and selectivity. Unlike the existing methods used for the detection of Phe, the proposed sensors provide multiplexed detection of a panel of metabolites without the need for complex sample preparations. The sensor cells were also implemented in a portable microfluidic device to enable the testing of various samples simultaneously on a single platform to facilitate the immediate biomarker assessment for PKU patients in a high-throughput manner. However, suitable disinfectants should be used after the analysis to prevent the accidental release of genetically modified organisms.

■ ASSOCIATED CONTENT

Supporting Information

The Supporting Information is available free of charge at https://pubs.acs.org/doi/10.1021/acsabm.0c00590.

Experimental details on strain construction, microfluidic chip design, and details of fluorescence assays (PDF)

■ AUTHOR INFORMATION

Corresponding Author

Yi-Chun Yeh − *Department of Chemistry, National Taiwan Normal University, Taipei 11677, Taiwan;* orcid.org/0000-0002-8267-0360; Phone: +886277496117; Email: yichuny@ntnu.edu.tw; Fax: +886229324249

Authors

Li-Wen Hsu − *Department of Chemistry, National Taiwan Normal University, Taipei 11677, Taiwan*

Yu-Hsuan Lin − *Department of Chemistry, National Taiwan Normal University, Taipei 11677, Taiwan*

Jun-Yu Guo − *Institute of Applied Mechanics, National Taiwan University, Taipei 10617, Taiwan*

Chien-Fu Chen − *Institute of Applied Mechanics, National Taiwan University, Taipei 10617, Taiwan;* orcid.org/0000-0001-7459-1649

Yi-Ju Chou − *Institute of Applied Mechanics, National Taiwan University, Taipei 10617, Taiwan*

Complete contact information is available at: https://pubs.acs.org/10.1021/acsabm.0c00590

Notes

The authors declare no competing financial interest.

■ ACKNOWLEDGMENTS

This work was funded by the Ministry of Science and Technology of Taiwan under the project number 107-2113-M-003-013-MY3.

■ REFERENCES

(1) Somaraju, U. R.; Merrin, M. Sapropterin dihydrochloride for phenylketonuria. *Cochrane Database Syst. Rev.* **2015**, *2015*, CD008005.

(2) Janssen, P. A. J.; Leysen, J. E.; Megens, A. A. H. P.; Awouters, F. H. L. Does phenylethylamine act as an endogenous amphetamine in some patients? *Int. J. Neuropsychopharmacol.* **1999**, *2*, 229−240.

(3) Fonnesbeck, C. J.; McPheeters, M. L.; Krishnaswami, S.; Lindegren, M. L.; Reimschisel, T. Estimating the probability of IQ impairment from blood phenylalanine for phenylketonuria patients: a hierarchical meta-analysis. *J. Inherit. Metab. Dis.* **2013**, *36*, 757−766.

(4) Blau, N.; van Spronsen, F. J.; Levy, H. L. Phenylketonuria. *Lancet* **2010**, *376*, 1417−1427.

(5) Burgard, P.; Rey, F.; Rupp, A.; Abadie, V.; Rey, J. Neuropsychologic functions of early treated patients with phenylketonuria, on and off diet: results of a cross-national and cross-sectional study. *Pediatr. Res.* **1997**, *41*, 368−374.

(6) Kawabata, Y.; Yamashiro, T.; Kitazaki, Y.; Imasaka, T. Optode for 2-phenethylamine using calixarene as host molecule. *Sens. Actuators, B* **1995**, *29*, 135−139.

(7) Ortuño, J. A.; Olmos, J. M.; Torralba, E.; Molina, A. Sensing and characterization of neurotransmitter 2-phenylethylamine based on facilitated ion transfer at solvent polymeric membranes using different electrochemical techniques. *Sens. Actuators, B* **2016**, *222*, 930−936.

(8) Jańczyk, M.; Kutyła-Olesiuk, A.; Ceto, X.; del Valle, M.; Ciosek, P.; Wroblewski, W. Resolution of amino acid mixtures by an array of potentiometric sensors based on boronic acid derivative in a SIA flow system. *Sens. Actuators, B* **2013**, *189*, 179−186.

(9) Cohen, J. D.; Baldi, B. G.; Slovin, J. P. 13C6-[benzene ring]-indole-3-acetic acid: a new internal standard for quantitative mass spectral analysis of indole-3-acetic acid in plants. *Plant Physiol.* **1986**, *80*, 14−19.

(10) Kaur, H.; Halliwell, B. Aromatic hydroxylation of phenylalanine as an assay for hydroxyl radicals: measurement of hydroxyl radical formation from ozone and in blood from premature babies using improved HPLC methodology. *Anal. Biochem.* **1994**, *220*, 11−15.
(11) Meesters, R. J. W.; Wolfe, R. R.; Deutz, N. E. P. Application of liquid chromatography-tandem mass spectrometry (LC−MS/MS) for the analysis of stable isotope enrichments of phenylalanine and tyrosine. *J. Chromatogr. B* **2009**, *877*, 43−49.
(12) Yujiao, W.; Guoyan, W.; Wenyan, Z.; Hongfen, Z.; Huanwang, J.; Anjia, C. Chiral separation of phenylalanine and tryptophan by capillary electrophoresis using a mixture of β-CD and chiral ionic liquid ([TBA][l-ASP]) as selectors. *Biomed. Chromatogr.* **2014**, *28*, 610−614.
(13) Lin, C.; Jair, Y.-C.; Chou, Y.-C.; Chen, P.-S.; Yeh, Y.-C. Transcription factor-based biosensor for detection of phenylalanine and tyrosine in urine for diagnosis of phenylketonuria. *Anal. Chim. Acta* **2018**, *1041*, 108−113.
(14) Lin, Y.-K.; Yeh, Y.-C. Dual-signal microbial biosensor for the detection of dopamine without inference from other catecholamine neurotransmitters. *Anal. Chem.* **2017**, *89*, 11178−11182.
(15) Guo, K.-H.; Lu, K.-H.; Yeh, Y.-C. Cell-Based Biosensor with Dual Signal Outputs for Simultaneous Quantification of Phenylacetic Acid and Phenylethylamine. *ACS Synth. Biol.* **2018**, *7*, 2790−2795.
(16) Díaz, E.; Ferrández, A.; Prieto, M. A.; García, J. L. Biodegradation of aromatic compounds by Escherichia coli. *Microbiol. Mol. Biol. Rev.* **2001**, *65*, 523−569.
(17) Luengo, J. M.; García, J. L.; Olivera, E. R. The phenylacetyl-CoA catabolon: a complex catabolic unit with broad biotechnological applications. *Mol. Microbiol.* **2001**, *39*, 1434−1442.
(18) Yamashita, M.; Azakami, H.; Yokoro, N.; Roh, J. H.; Suzuki, H.; Kumagai, H.; Murooka, Y. maoB, a gene that encodes a positive regulator of the monoamine oxidase gene (maoA) in Escherichia coli. *J. Bacteriol.* **1996**, *178*, 2941−2947.
(19) Ferrández, A.; Miñambres, B.; García, B.; Olivera, E. R.; Luengo, J. M.; García, J. L.; Díaz, E. Catabolism of phenylacetic acid in Escherichia coli. *J. Biol. Chem.* **1998**, *273*, 25974−25986.
(20) Hanlon, S. P.; Hill, T. K.; Flavell, M. A.; Stringfellow, J. M.; Cooper, R. A. 2-Phenylethylamine catabolism by Escherichia coli K-12: gene organization and expression. *Microbiology* **1997**, *143*, 513−518.
(21) Pittard, J.; Camakaris, H.; Yang, J. The TyrR regulon. *Mol. Microbiol.* **2004**, *55*, 16−26.
(22) Koyanagi, T.; Katayama, T.; Suzuki, H.; Kumagai, H. Altered oligomerization properties of N316 mutants of Escherichia coli TyrR. *J. Bacteriol.* **2008**, *190*, 8238−8243.
(23) Neuwald, A. F.; Aravind, L.; Spouge, J. L.; Koonin, E. V. AAA+: A class of chaperone-like ATPases associated with the assembly, operation, and disassembly of protein complexes. *Genome Res.* **1999**, *9*, 27−43.
(24) Sarsero, J. P.; Pittard, A. J. Molecular analysis of the TyrR protein-mediated activation of mtr gene expression in Escherichia coli K-12. *J. Bacteriol.* **1991**, *173*, 7701−7704.
(25) Pittard, A. J.; Davidson, B. E. TyrR protein of Escherichia coli and its role as repressor and activator. *Mol. Microbiol.* **1991**, *5*, 1585−1592.
(26) Andrews, A. E.; Lawley, B.; Pittard, A. J. Mutational analysis of repression and activation of the tyrP gene in Escherichia coli. *J. Bacteriol.* **1991**, *173*, 5068−5078.
(27) Andrews, A. E.; Dickson, B.; Lawley, B.; Cobbett, C.; Pittard, A. J. Importance of the position of TYR R boxes for repression and activation of the tyrP and aroF genes in Escherichia coli. *J. Bacteriol.* **1991**, *173*, 5079−5085.
(28) Yang, J.; Hwang, J. S.; Camakaris, H.; Irawaty, W.; Ishihama, A.; Pittard, J. Mode of action of the TyrR protein: repression and activation of the tyrP promoter of Escherichia coli. *Mol. Microbiol.* **2004**, *52*, 243−256.
(29) Wang, P.; Yang, J.; Pittard, A. J. Promoters and transcripts associated with the aroP gene of Escherichia coli. *J. Bacteriol.* **1997**, *179*, 4206−4212.
(30) Chen, J.-Y.; Huang, Y.-T.; Chou, H.-H.; Wang, C.-P.; Chen, C.-F. Rapid and inexpensive blood typing on thermoplastic chips. *Lab Chip* **2015**, *15*, 4533−4541.
(31) Ferrández, A.; García, J. L.; Díaz, E. Transcriptional Regulation of the Divergent paaCatabolic Operons for Phenylacetic Acid Degradation inEscherichia coli. *J. Biol. Chem.* **2000**, *275*, 12214−12222.
(32) Wang, B.; Kitney, R. I.; Joly, N.; Buck, M. Engineering modular and orthogonal genetic logic gates for robust digital-like synthetic biology. *Nat. Commun.* **2011**, *2*, 508.
(33) Williams, R. A.; Mamotte, C. D.; Burnett, J. R. Phenylketonuria: an inborn error of phenylalanine metabolism. *Clin. Biochem. Rev.* **2008**, *29*, 31.
(34) Vermeulen, N.; Gánzle, M. G.; Vogel, R. F. Influence of peptide supply and cosubstrates on phenylalanine metabolism of Lactobacillus sanfranciscensis DSM20451T and Lactobacillus plantarum TMW1. 468. *J. Agric. Food Chem.* **2006**, *54*, 3832−3839.

https://dx.doi.org/10.1021/acsabm.0c00590
ACS Appl. Bio Mater. XXXX, XXX, XXX−XXX